International Journal of Solids and Structures 50 (2013) 2542–2547

Contents lists available at SciVerse ScienceDirect

International Journal of Solids and Structures

journal homepage: www.elsevier.com/locate/ijsolstr

Orientation effect on the Boussinesq indentation of a transversely isotropic piezoelectric material

Ming Liu, Fuqian Yang *

Materials Program, Department of Chemical and Materials Engineering, University of Kentucky, Lexington 40506, USA

ARTICLE INFO

Article history:
Received 30 October 2012
Received in revised form 18 March 2013
Available online 19 April 2013

Keywords:
Indentation deformation
Piezoelectric materials
3-D FEM simulation
Load-displacement relation

ABSTRACT

Three-dimensional finite element analysis was used to study the effect of the angle between the loading direction and the axisymmetric direction on the indentation behavior of a transversely isotropic piezoelectric half-space by a cylindrical indenter of flat end. Two cases were considered in the analysis, which included (a) the indentation by an insulating indenter, and (b) the indentation by a conducting indenter. Both the indentation load and the indentation-induced potential were found to be proportional to the indentation depth. Using the simulation results and the analytical relationship for the indentation by a rigid, insulating indenter, semi-analytical relationships were developed between the indentation load and the indentation depth and between the indentation-induced potential on the indenter and the indentation depth for the conducting indenter, respectively. The proportionality between the indentation-induced potential and the indentation depth is only a function of the angle between the loading direction and the poling direction, independent of the type of indenters, which may be used to measure the relative direction of the loading axis to the axisymmetric axis of transversely piezoelectric materials from the indentation test.

1. Introduction

With the extensive applications of piezoelectric materials in sensors, actuators, and smart structures of small volume, there is a great need to understand the electromechanical behavior of piezoelectric materials for quality control and performance prediction. Various techniques have been developed to characterize mechanical properties of materials, which include indentation technique (Alguero et al., 2001; Kamble et al., 2009; Nili et al., 2013; Ramamurty et al., 1999; Rar et al., 2006; Song et al., 2012; Sridhar et al., 1999; Wong and Zeng, 2008; Yang, 2008a; Yang and Dang, 2009; Zhao et al., 2012), piezoresponse force microscopy (Dunn and Whatmore, 2001; Kalinin et al., 2004; Schneider et al., 2005; Yang, 2008a), and atomic force microscopy (Schneider et al., 2005; Yang, 2008a; Zeng et al., 2011). In the heart of the contact technique is the relationship between the indentation load and the indentation depth, which depends on the properties of materials.

Matysiak (1985) was the first to analyze the axisymmetric contact of a transversely isotropic piezoelectric half-space. Giannakopoulos and Suresh (1999) used Matysiak's approach (1985) to present a general solution for the axisymmetric indentation of a transversely isotropic piezoelectric half-space. Using the potential theory, Ding et al. (2000) obtained analytical solutions of the stress and electric fields for the indentation of a transversely isotropic piezoelectric half-space by a spherical indenter, a conical indenter, and an upright circular flat indenter. Yang (2004) studied the electromechanical coupling between a compliant surface electrode and a transversely isotropic piezoelectric half-space. Yang (2008b) obtained the contact stiffness, effective piezoelectric constant and electric displacement intensity factor for the axisymmetric indentation of a semi-infinite piezoelectric material by a rigid, conducting indenter of arbitrary-axisymmetric profile. Wang and Chen (2011) considered the indentation response of a piezoelectric film bonded to an elastic substrate by an axisymmetrical indenter and reduced the indentation problem to the solution of a dual integral equation. Wu et al. (2012) reduced the solution for the indentation of a piezoelectric film on an elastic film to a Fredholm integral equation of the second kind and solved the problem numerically.

Due to the complexity of electromechanical interaction, finite element methods have been used to analyze the contact deformation of piezoelectric materials. Wang and Han (2006) analyzed the indentation of a piezoelectric layer by a flat-ended cylindrical indenter and numerically simulated the deformation of the piezoelectric layer indented. Giannakopoulos (2000) incorrectly used zero electric potential on the axisymmetric axis in the finite element analysis of the spherical indentation of piezoelectric materials. Kamble et al. (2009) applied the same condition used by Giannakopoulos (2000) in the finite element analysis of the spherical indentation of polycrystalline PZT-4. Liu and Yang

* Corresponding author. Tel.: +1 859 257 2994; fax: +1 859 323 1929.
E-mail address: fyang0@engr.uky.edu (F. Yang).

0020-7683/$ - see front matter © 2013 Elsevier Ltd. All rights reserved.
http://dx.doi.org/10.1016/j.ijsolstr.2013.04.004

(2012) used the finite element method to examine the effect of surface electric conditions on the spherical indentation of transversely isotropic piezoelectric materials without applying electric condition to the axisymmetric axis. Using axisymmetric and 3-D finite element simulations, Zhao (2011) recently studied the effect of poling direction and indenter size on the indentation of PZT-5H by a flat-ended cylindrical indenter in which only one case with the indentation direction being not parallel to the poling direction was shown. No detailed study was given to the effect of crystal orientation.

It is worth mentioning piezoelectric ceramics are brittle and it will be difficult to indent them without creating surface cracks. Ramamurty et al. (1999) assumed elastic response of the indentation of PZT-4 and used the loading curves to measure the indentation stiffness. There is only about 10–15% difference between the measured results and the calculation results. Their results suggest that it is possible to use the indentation loading curve to approximately determine the mechanical properties of piezoelectric ceramics.

Piezoelectric interaction depends on crystal orientation, and the effect of material anisotropy on indentation response requires detailed study. When the direction of indentation loading is not aligned with the poling direction, axisymmetric analysis cannot suffice. Asymmetric analysis is needed to understand the effect of material anisotropy including stiffness and piezoelectric responses associated with crystal orientation. Three-dimensional finite element analysis has been widely used for investigating anisotropic structures (Cox et al., 1994; Cheng and Venkatesh, 2012) in which analytical solutions are deficient. In this work, three-dimensional finite element analysis of the Boussinesq indentation of transversely isotropic piezoelectric materials is performed. The study is aimed at analyzing the effect of material anisotropy on the relationship between indentation load and indentation depth and that between indentation-induced potential and indentation depth.

2. Problem formulation and finite element model

For transversely isotropic piezoelectric materials, the constitutive relations are

$$\sigma_{ij} = C^E_{ijkl}\varepsilon_{kl} - e_{ijk}E_k \tag{1}$$

$$D_i = e_{ikl}\varepsilon_{kl} + \in^E_{ij} E_j \tag{2}$$

where σ_{ij} ($i, j = 1, 2, 3$) are the components of stress tensor, ε_{ij} are the components of strain tensor, D_i are the components of electric displacement vector, E_i are the components of electric field intensity, C^E_{ijkl} are the components of the elastic stiffness tensor measured in a constant electric field intensity, e_{ijk} are the components of the piezoelectric tensor measured in possession of a spontaneous electric field and $\in^E_{ij}$ are the components of dielectric tensor. The relation between the components of the strain tensor ε_{ij} and the components of the displacement vector u_i is

$$\varepsilon_{ij} = \frac{1}{2}\left(\frac{\partial u_i}{\partial x_j} + \frac{\partial u_j}{\partial x_i}\right) \tag{3}$$

and the relation between the components of the electric field intensity E_i and electric potential ϕ is

$$E_i = -\frac{\partial \phi}{\partial x_i} \tag{4}$$

The equilibrium equations are

$$\sum_{j=1}^{3} \frac{\partial \sigma_{ij}}{\partial x_j} = 0 \quad (i = 1, 2, 3) \tag{5}$$

Without any free electric charge in the piezoelectric material, there is

$$\frac{\partial D_1}{\partial x_1} + \frac{\partial D_2}{\partial x_2} + \frac{\partial D_3}{\partial x_3} = 0 \tag{6}$$

Consider the indentation of a linear piezoelectric half-space ($z > 0$) by a rigid, cylindrical indenter of flat end. The loading direction is parallel to the surface normal of the piezoelectric material, and let the angle between the loading direction and the poling direction (axisymmetric axis) be θ.

The mechanical boundary conditions for the indentation are

$$\sigma_{rz}(r, \vartheta, 0) = 0 \tag{7}$$

$$\sigma_{zz}(r, \vartheta, 0) = 0 \quad \text{for } r > a \tag{8}$$

$$u_z(r, \vartheta, 0) = \delta \quad \text{for } r < a \tag{9}$$

where δ is the indentation depth, and a is the contact radius the same as the radius of the indenter. Eq. (7) represents frictionless contact between the indenter and the piezoelectric material, and Eq. (8) indicates stress-free condition outside the contact zone. The indentation load, F, can be calculated from the force balance on the indenter as

$$F = -\int_0^{2\pi}\int_0^a \sigma_{zz}(r, \vartheta, 0) r dr d\vartheta \tag{10}$$

where ϑ is the azimuth angle between a reference line and the r-axis.

The conditions at infinity require

$$u_r(r, \vartheta, z) = u_z(r, \vartheta, z) = 0 \text{ and } \phi(r, \vartheta, z) = 0 \text{ for } \sqrt{r^2 + z^2} \to \infty \tag{11}$$

Two types of indenters are used in the analysis. They are as follows.

Case I. Insulating indenter

The electric boundary condition on the surface of the piezoelectric material for the indentation by an insulating indenter is

$$D_z(r, \vartheta, 0) = 0 \quad \text{for } r \geqslant 0 \tag{12}$$

where D_z is the z-component of the electric displacement vector.

Case II. Conducting indenter

According to the direct piezoelectric effect, the indentation deformation will create an electric field in the piezoelectric material and a uniform electric potential over the contact zone by a conducting indenter (Liu and Yang, 2012). The electric potential is dependent on the indentation depth to be determined from solving the indentation deformation. The electric boundary conditions on the surface of the piezoelectric material are

$$D_z(r, \vartheta, 0) = 0 \quad \text{for } r > a \tag{13}$$

$$\phi(r, \vartheta, 0) = \phi_c \quad \text{for } r < a \tag{14}$$

with ϕ_c being the indentation-induced electric potential on the indenter, which is to be determined from solving the contact deformation.

In the simulation, transversely isotropic piezoelectric materials are used since most polycrystalline, poled piezoelectric materials conform to this symmetry group (Ramamurty et al., 1999). Table 1 lists the material properties used in the simulation, which are referenced to the intrinsic material coordinate with the poling direction the same as the axisymmetric axis of the materials. Note that both elastic constants and piezoelectric constants are presented in the matrix form instead of the tensor form.

The analysis of the indentation deformation uses the large elastoplastic feature of the ABAQUS finite element code. The contact radius, a, between the indenter and the piezoelectric material is 100 nm. The piezoelectric material is modeled as a cylinder with 1000 nm in height and 1000 nm in radius, which is 10 times the contact radius. Under such a geometrical condition, the

Table 1
Material properties of transversely isotropic piezoelectric ceramics.

	Elastic constant (10^{10} N/m^2)					Piezoelectric constant (C/m^2)			Dielectric constant (10^{-10} C/V m)	
	c_{11}	c_{12}	c_{13}	c_{33}	c_{44}	e_{31}	e_{33}	e_{15}	$\in_{11}$	$\in_{33}$
PZT-4 [28, 29]	13.9	7.78	7.43	11.3	2.56	−6.98	13.84	13.44	60.0	54.7
$BaTiO_3$ [15]	16.6	7.66	7.75	16.2	4.29	−4.4	18.6	11.6	111.51	125.67

piezoelectric material can be approximately treated as semi-infinite. To avoid possible convergence problems arising from the sharp edge of the indenter, a rigid indenter with a flat end but around edge of 0.2 nm in radius is used, whose effect is negligible because of the ratio of the radius of the rounded edge to the diameter of the indenter being less than 1% (Yang, 1998). The finite element mesh, shown in Fig. 1, consists of 36,297 8-node linear piezoelectric bricks with mesh refinement around the contact zone.

The indenter is modeled as a rigid surface, and the contact between the indenter and the piezoelectric material is assumed as frictionless. The bottom surface of the piezoelectric material is fixed and electrically grounded. Displacement-controlled indentation is used in the simulation. The indenter is gradually pushed onto the surface of the piezoelectric material to a preset depth, and then it is withdrawn until the load on the indenter becomes zero.

3. Results and discussion

3.1. Load–displacement relationship

From the indentation load–displacement curves, one can determine the contact stiffness and the contact modulus, which depend on the material properties. Fig. 2 shows the variation of the indentation load with the indentation depth for the indentation of PZT-4 with various angles between the loading direction and the axisymmetric axis (the poling direction). The indentation load increases linearly with increasing the indentation depth, independent of the angle θ, while the ratio of F/δ depends on the angle θ and the type of indenters. It is interesting to note that the ratio of the indentation load to the indentation depth, F/δ, for $\theta = 0^o$ is independent of the type of indenters, i.e. the indentation by a conducting indenter (case II) or by an insulating indenter (case I) produces the same indentation load–displacement curves when the loading direction is parallel to the axisymmetric axis.

Wang et al. (2008) had summarized the relationship between the indentation load and the indentation depth for the axisymmetric indentation of transversely isotropic piezoelectric semi-infinite materials by an insulating indenter of flat end, which corresponds to the condition of $\theta = 0^o$. The dependence of the indentation load on the indentation displacement can be expressed as (Giannakopoulos and Suresh, 1999; Wang et al., 2008)

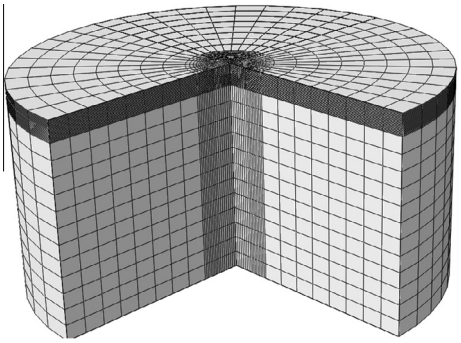

Fig. 1. Finite element mesh for the indentation of a piezoelectric half-space.

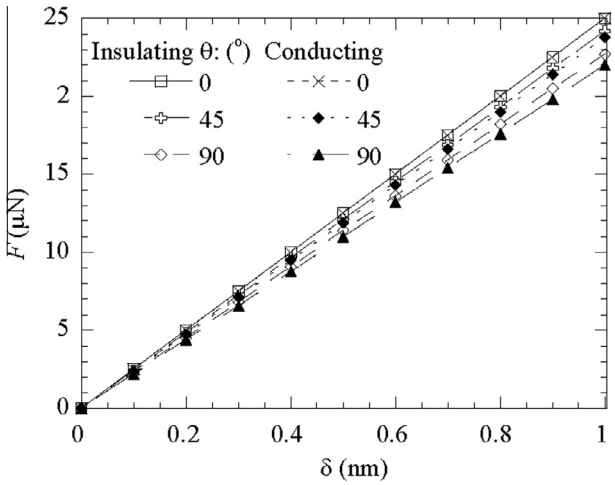

Fig. 2. Dependence of the indentation load on the indentation depth for the indentation of PZT-4 with various angles between the loading direction and the poling direction.

$$F = 4a\delta\frac{M_6M_7 - M_5M_8}{M_1M_8 - M_2M_7} \tag{15}$$

where M_i $(i = 1, 2, \ldots, 8)$ are dependent on the material properties of the piezoelectric material (Giannakopoulos and Suresh, 1999; Wang et al., 2008). Using the data in Table 1, one can obtain the dependence of the indentation load on the indentation depth as $F = 22.864 \times 10^{10} a\delta$ in which the unit of a and δ is millimeter and the unit of F is Newton. For the same indentation depth, the percent difference of the indentation load between the results calculated from the finite element analysis and the analytical results is ~7%, suggesting that the finite element mesh is good enough for the three-dimensional analysis of the Boussinesq indentation of a transversely isotropic piezoelectric material.

Fig. 3 shows the variation of the ratio F/δ with the angle θ for the indentation of PZT-4 by conducting and insulating indenters. Independent of the type of indenters, the ratio starts with a maximum value at $\theta = 0°$, decreases to the minimum value at $\theta = 90°$, and then increases to the maximum value at $\theta = 180°$. The indentation response, i.e. the ratio of F/δ, follows the same behavior for the angle of θ in range of 180–360°. Generally, the ratio for the indentation by an insulating indenter is larger than that by a conducting indenter.

The simulation results for the indentation deformation of $BaTiO_3$ is also included in Fig. 3 for the variation of F/δ with θ. Obviously the dependence of F/δ on θ follows a similar trend. Thus, one might suggest that such behavior also applies to other transversely isotropic piezoelectric materials, and the relationship between the ratio of F/δ and θ (in the unit of degree) can be expressed as

$$\frac{F}{\delta} = 4a\frac{M_6M_7 - M_5M_8}{M_1M_8 - M_2M_7} f(\theta, c_{ij}, e_{ij}, \in_{ij}) \tag{16}$$

with $f(\theta, c_{ij}, e_{ij}, \in_{ij})$ as

$$f(\theta, c_{ij}, e_{ij}, \in_{ij}) = \alpha + \beta\cos\frac{\pi\theta}{90} \tag{17}$$

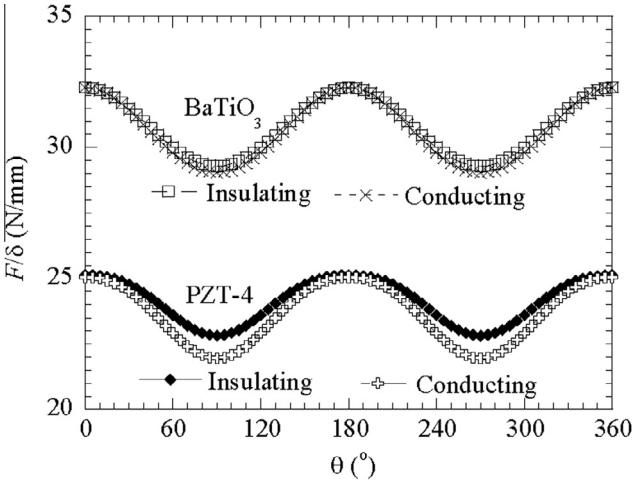

Fig. 3. Variation of the ratio of F/δ with the angle θ for PZT-4 and $BaTiO_3$.

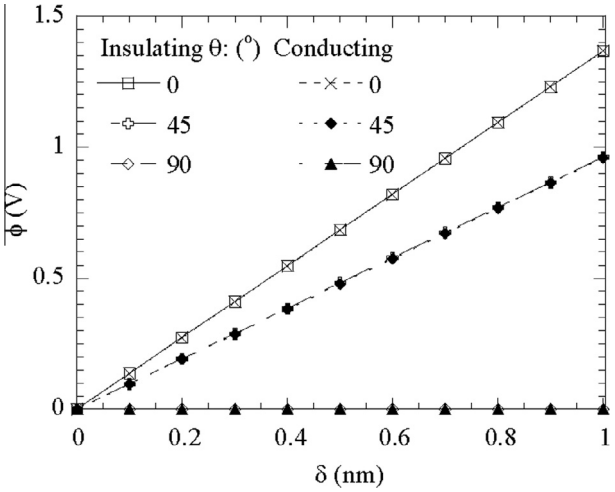

Fig. 4. Dependence of the indentation-induced electric potential at the contact center on the indentation depth for the indentation of PZT-4 with various angles between the loading direction and the poling direction.

Here, α is a constant related to the indentation response of the piezoelectric material at $\theta = 45°$ and β is a constant dependent on material properties and electric boundary conditions. Table 2 lists the values of α and β for the materials of PZT-4 and $BaTiO_3$, which are obtained from the best curve-fitting. Note that $\alpha + \beta = 1$ in accord with Eq. (17) at $\theta = 0°$.

From Eq. (16), the contact stiffness for the indentation of a transversely isotropic piezoelectric half-space by a rigid, cylindrical indenter of flat end can be calculated as

$$\frac{dF}{d\delta} = 4a\frac{M_6M_7 - M_5M_8}{M_1M_8 - M_2M_7}\left(\alpha + \beta\cos\frac{\pi\theta}{90}\right) = 4\sqrt{\frac{A}{\pi}}\frac{M_6M_7 - M_5M_8}{M_1M_8 - M_2M_7}\left(\alpha + \beta\cos\frac{\pi\theta}{90}\right) \tag{18}$$

where A is the contact area. The contact stiffness is proportional to the square root of the contact area, and the proportionality is dependent on the piezoelectric properties of materials and the electric boundary conditions. Eq. (18) is the same as that for the indentation by a rigid, spherical indenter when $\theta = 0°$ (Giannakopoulos and Suresh, 1999; Wang et al., 2008).

3.2. Electric potential–displacement relationship

The variation of the indentation-induced electric potential at the contact center with the indentation depth is shown in Fig. 4 for the indentation of PZT-4 with various angles between the loading direction and the axisymmetric axis (the poling direction). Note that the electric potential within the contact region for the indentation by the conducing indenter is not pre-determined and is the same as the indentation-induced potential on the indenter. The indentation-induced potential linearly increases with increasing the indentation depth. For the same indentation depth, there is no difference between the indentation-induced potential in the contact zone by a rigid, conducting indenter and that at the contact center by a rigid, insulating indenter for all the angles shown in Fig. 4.

Fig. 5 shows the variation of the ratio $\phi(0,0)/\delta$ with the angle θ for the indentation of PZT-4 by conducting and insulating indenters. Obviously, the indentation-induced potential at the contact center by the rigid, insulating indenter is the same as the indentation-induced potential on the conducting indenter. The reason can be explained by the closed-form solution of the electric potential that insulating indenter creates a constant electric potential inside the contact area for flat-ended indenter (Giannakopoulos and Suresh, 1999; Wang et al., 2008), which is just the same electric potential constraint as that for the conducting indenter. For the indentation of a transversely isotropic piezoelectric half-space by a rigid, insulating indenter, the indentation-induced potential over the contact zone for $\theta = 0°$ can be expressed as (Giannakopoulos and Suresh, 1999; Wang et al., 2008)

$$\phi = \delta\frac{M_3M_8 - M_4M_7}{M_1M_8 - M_2M_7} \quad \text{for } r < a \tag{19}$$

which is independent of the radial variable and satisfies the condition of Eq. (14). This suggests that the indentation-induced potential by a rigid, cylindrical indenter of flat end is insensitive to the

Table 2
Numerical values of α and β for the materials of PZT-4 and $BaTiO_3$.

	α	β
PZT-4 (IP)	0.954	0.046
PZT-4 (CP)	0.94	0.06
$BaTiO_3$ (IP)	0.954	0.046
$BaTiO_3$ (CP)	0.948	0.052

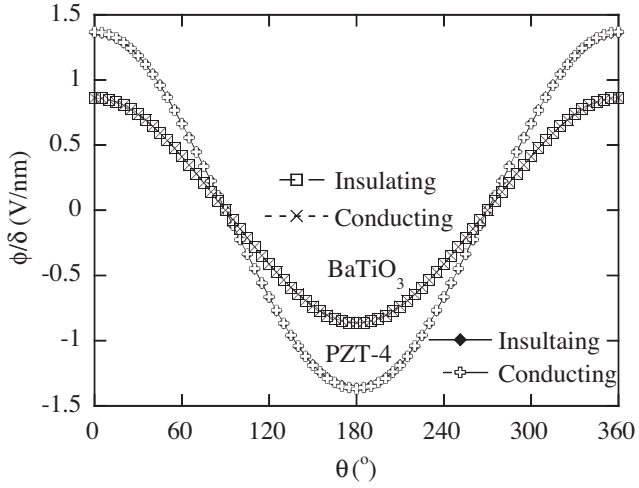

Fig. 5. Variation of the ratio of ϕ/δ with the angle θ for PZT-4 and $BaTiO_3$.

type of indenters for $\theta = 0°$. Eq. (19) can be used to describe the indentation-induced potential on the conducting indenter of flat end for the axisymmetric indentation of a transversely isotropic piezoelectric half-space. It is worth mentioning that the uniform distribution of the electric potential over the contact area for the indentation by an insulating indenter of flat end only occurs for $\theta = 0°$.

As shown in Fig. 5, the ratio $\phi(0,0)/\delta$ starts with a maximum value at $\theta = 0°$, decreases to the minimum value at $\theta = 180°$, and then increases to the maximum value at $\theta = 360°$. The simulation results for the indentation deformation of $BaTiO_3$ are also included in Fig. 5 for the variation of $\phi(0,0)/\delta$ with θ. Obviously the variation of ϕ/δ with θ follows a similar trend as that for the indentation of PZT-4. Thus, such behavior might also apply to other transversely piezoelectric materials. Note that the sign of the ratio ϕ/δ changes from a positive value to a negative value when the relative direction between the poling direction and the loading direction changes from 0° to 180°; and the ratio $\phi(0,0)/\delta$ is zero at $\theta = 90°$ and 270°. As expected, the indentation-induced potential with the loading direction opposite to the poling direction has the same absolute magnitude as that with the loading direction the same as the poling direction. This is because the piezoelectric constants reverse their sign while the elastic and dielectric constants remain unaltered due to polarization switching (Kamble et al., 2009). Based on the discussion, one can express the relationship between the ratio of ϕ/δ and θ (in the unit of degree) for the indentation by a rigid, conducting indenter of flat end as

$$\frac{\phi}{\delta} = \frac{M_3M_8 - M_4M_7}{M_1M_8 - M_2M_7}\cos\frac{\pi\theta}{180} \quad \text{for } r < a \tag{20}$$

which can be used to quantify the relative direction between the loading axis and the poling direction from the indentation test.

Understanding the contact deformation of piezoelectric materials represents an important research topic in improving the structural applications of piezoelectric materials. As the contact size decreases to submicron scale, contact adhesion likely becomes important. Using the Dugdale model, Chen and Yu (2005) studied the adhesive contact between a rigid spherical indenter and a piezoelectric half-space. Rogowski and Kalinski (2007) analyzed the adhesive contact between a rigid indenter of flat end and a piezoelectric half-space. Guo and Jin (2009) examined the two-dimensional adhesive contact between a transversely isotropic half-space and a rigid cylinder. The intrinsic assumption used in their analyses (Chen and Yu, 2005; Rogowski and Kalinski, 2007) was that the contact shape is similar during the separation of the indenter from the piezoelectric material. Such an assumption has been used in studying the adhesive contact of elastic, isotropic materials (Johnson et al., 1971; Yang and Li, 2001) and is plausible for the loading axis is parallel to the axisymmetric axis of piezoelectric materials. For the indentation of piezoelectric materials with the loading axis being not parallel to the axisymmetric axis, it is unclear if the contact shape is similar for the adhesive contact. Also the contribution of surface energy to the adhesive contact of piezoelectric ceramics generally is negligible due to large elastic constants, while the capillary effect likely will become important for the contact adhesion. Under such a condition, different boundary conditions need to be used and new solution needs to be derived.

There are several reports on the indentation-induced domain switching in ferroelectric materials (Busche and Hsia, 2001; Cheng et al., 2008; Deluca et al., 2010), including PZT-4 ceramic. It has been pointed out by Busche and Hsia (2001) that "the stress level alone is not sufficient to induce domain switch" and the local stress with the sign favoring switching possibly determines the domain switching. However, it is impossible to quantitatively analyze the indentation-induced domain switching without including the stress-induced domain switching in the constitutive relationship. The contact mechanics of the piezoelectric materials with the stress-induced domain switching is complicated and needs to be further studied by introducing the terms related to the stress-induced domain switching.

4. Summary

Stress and electric fields play an important role in controlling the electromechanical coupling of piezoelectric materials. A three-dimensional finite element model was built to analyze the indentation behavior of a transversely isotropic piezoelectric half-space by a rigid, cylindrical indenter of flat end, aiming at examining the effect of the angle between the loading direction and the poling direction on the indentation response of piezoelectric materials. Two types of indenters were used in the analysis: one was a conducting indenter and the other an insulating indenter.

The finite element results revealed that both the indentation load and the magnitude of the indentation-induced potential linearly increase with increasing the indentation depth. The proportionality for the linear relationship between the indentation load and the indentation depth depends on the angle, type of indenters, and piezoelectric properties of materials. In contrast to the load–displacement relationship, the proportionality for the linear relationship between the indentation-induced potential and the indentation depth is only a function of the angle between the loading direction and the poling direction, independent of the type of indenters. Semi-analytical relationships were established between the indentation load and the indentation depth and between the indentation-induced potential and the indentation depth. These relationships may be used in the indentation technique to measure the relative direction of the loading axis to the poling direction (axisymmetric axis) of transversely isotropic piezoelectric materials.

This work provides a simple relation between the loading direction and the poling direction for the indentation of transversely isotropic piezoelectric materials. In general, it is worth comparing the simulation results to experimental results, in which the indentation direction is different from the poling direction. This requires experimental study to examine the effect of the poling direction on the indentation behavior of piezoelectric materials.

Acknowledgments

This work is supported by the NSF through Grant No CMMI-0800018. The authors would like to thank the University of Kentucky Information Technology Department and Center for Computational Sciences for computing time on the Lipscomb High Performance Computing Cluster. This research was supported in part by the NSF through XSEDE resources provided by SDSC (National allocation).

References

Alguero, M., Bushby, A.J., Hvizdos, P., Reece, M.J., Whatmore, R.W., Zhang, Q., 2001. Mechanical and electromechanical properties of PZT sol-gel thin films measured by nanoindentation. Integr. Ferroelectr. 41, 1705–1714.
Busche, M.J., Hsia, K.J., 2001. Fracture and domain switching by indentation in barium titanate single crystals. Scr. Mater. 44, 207–212.
Chen, Z.R., Yu, S.W., 2005. Micro-scale adhesive contact of a spherical rigid punch on a piezoelectric half-space. Compos. Sci. Technol. 65, 1372–1381.
Cheng, G., Venkatesh, T.A., 2012. Nanoindentation response of anisotropic piezoelectric materials. Philos. Mag. Lett. 92, 278–287.
Cheng, S.Y., Ho, N.J., Lin, H.Y., 2008. Micro-indentation-induced domain switching in tetragonal barium titanate. J. Am. Ceram. Soc. 91, 3721–3727.
Cox, B.N., Carter, W.C., Fleck, N.A., 1994. A binary model of textile composites–I. Formulation. Acta Metall. Mater. 42, 3463–3479.

Deluca, M., Bermejo, R., Grünbichler, H., Presser, V., Danzera, R., Nickel, K.G., 2010. Raman spectroscopy for the investigation of indentation-induced domain texturing in lead zirconate titanate piezoceramics. Scr. Mater. 63, 343–346.
Ding, H.J., Hou, P.F., Gou, F.L., 2000. The elastic and electric fields for three dimensional contact for transversely isotropic piezoelectric materials. Int. J. Solids Struct. 37, 3201–3229.
Dunn, S., Whatmore, R.W., 2001. Transformation dependence of lead zirconate titanate (PZT) as shown by PiezoAFM surface mapping of Sol-gel produced PZT on various substrates. Integr. Ferroelectr. 38, 683–691.
Giannakopoulos, A.E., 2000. Strength analysis of spherical indentation of piezoelectric materials. J. Appl. Mech. 67, 409–416.
Giannakopoulos, A.E., Suresh, S., 1999. Theory of indentation of piezoelectric materials. Acta Mater. 47, 2153–2164.
Guo, X., Jin, F., 2009. A generalized JKR-model for two-dimensional adhesive contact of transversely isotropic piezoelectric half-space. Int. J. Solids Struct. 46, 3607–3619.
Johnson, K.L., Kendall, K., Roberts, A.D., 1971. Surface energy and contact of elastic solids. Proc. R. Soc. London A 324, 301–313.
Kamble, S.N., Kubair, D.V., Ramamurty, U., 2009. Indentation strength of a piezoelectric ceramic: experiments and simulations. J. Mater. Res. 24, 926–935.
Kalinin, S.V., Karapetian, E., Kachanov, M., 2004. Nanoelectromechanics of piezoresponse force microscopy. Phys. Rev. B 70, 184101.
Liu, M., Yang, F.Q., 2012. Finite element analysis of the spherical indentation of transversely isotropic piezoelectric materials. Modell. Simul. Mater. Sci. Eng. 20, 045019.
Matysiak, S., 1985. Axisymmetric problem of punch pressing into a piezoelectroelastic halfspace. Bull. Pol. Acad. Sci. Technol. Sci. 33, 25–33.
Nili, H., Cheng, G., Venkatesh, T.A., Sriram, S., Bhaskaran, M., 2013. Correlation between nanomechanical and piezoelectric properties of thin films: an experimental and finite element study. Mater. Lett. 90, 148–151.
Ramamurty, U., Sridhar, S., Giannakopoulos, A.E., Suresh, S., 1999. An experimental study of spherical indentation on piezoelectric materials. Acta Mater. 47, 2417–2430.
Rar, A., Pharr, G.M., Oliver, W.C., Karapetian, E., Kalinin, S.V., 2006. Piezoelectric nanoindentation. J. Mater. Res. 21, 552–556.
Rogowski, B., Kalinski, W., 2007. The adhesive contact problem for a piezoelectric half-space. Int. J. Press. Vessels Pip. 84, 502–511.
Schneider, G.A., Scholz, T., Munoz-Saldana, J., Swain, M.V., 2005. Domain rearrangement during nanoindentation in single-crystalline barium titanate measured by atomic force microscopy and piezoresponse force microscopy. Appl. Phys. Lett. 86, 192903.
Song, S.T., Zheng, X.J., Zheng, H., Liu, W., 2012. Evaluation of engineering/piezoelectric constants of piezoelectric thin film by combining nanoindentation test with FEM. Comput. Mater. Sci. 63, 134–144.
Sridhar, S., Giannakopoulos, A.E., Suresh, S., Ramamurty, U., 1999. Electrical response during indentation of piezoelectric materials: a new method for material characterization. J. Appl. Phys. 85, 380–387.
Wang, J.H., Chen, C.Q., 2011. Indentation responses of piezoelectric films ideally bonded to an elastic substrate. Int. J. Solids Struct. 48, 2743–2754.
Wang, J.H., Chen, C.Q., Lu, T.J., 2008. Indentation responses of piezoelectric films. J. Mech. Phys. Solids 56, 3331–3351.
Wang, B.L., Han, J.C., 2006. A circular indenter on a piezoelectric layer Arch. Appl. Mech. 76, 367–379.
Wong, M.F., Zeng, K., 2008. Deformation behavior of PZN-6%PT single crystal during nanoindentation. Philos. Mag. 88, 3105–3128.
Wu, Y.F., Yu, H.Y., Chen, W.Q., 2012. Mechanics of indentation for piezoelectric thin films on elastic substrate. Int. J. Solids Struct. 49, 95–110.
Yang, F.Q., 1998. Impression creep: effects of slip, stick and cavity depth. Int. J. Mech. Sci. 40, 87–96.
Yang, F.Q., 2004. Electromechanical interaction of linear piezoelectric materials with a surface electrode. J. Mater. Sci. 39, 2811–2820.
Yang, F.Q., 2008a. Piezoelectric response in the contact deformation of piezoelectric materials. In: Yang, F.Q., Li, J.C.M. (Eds.), Micro and Nano Mechanical Testing of Materials and Devices. Springer, pp. 155–178.
Yang, F.Q., 2008b. Analysis of the axisymmetric indentation of a semi-infinite piezoelectric material: The evaluation of the contact stiffness and the effective piezoelectric constant. J. Appl. Phys. 103, 074115.
Yang, F.Q., Dang, H.M., 2009. Effect of electric field on the nanoindentation of Zinc Sulfide. J. Appl. Phys. 105, 056110.
Yang, F.Q., Li, J.C.M., 2001. Adhesion of a rigid punch to an incompressible elastic film. Langmuir 17, 6524–6529.
Zeng, H., Wu,, P., Dong, D.X., Zhang, P., 2011. Investigation on preparation and properties of Pb(Zr0.95Ti0.05)O-3 thin films. Infrared Phys. Technol. 54, 21–24.
Zhao, B., 2011. Determination of mechanics properties of a piezoelectric material suing indentation method with a cylindrical indenter. Adv. Mater. Res. 335–336, 1014–1020.
Zhao, G.F., Liu, M., Yang, F.Q., 2012. The effect of an electric current on the nanoindentation behavior of tin. Acta Mater. 60, 3773–3782.